Arabian Journal of Chemistry (2023) **16**, 104626

King Saud University

Arabian Journal of Chemistry

www.ksu.edu.sa
www.sciencedirect.com

ORIGINAL ARTICLE

Synthesis characterization and evaluation of novel triazole based analogs as a acetylcholinesterase and α-glucosidase inhibitors

Hafiz M. A. Asif [a], Shagufta Kamal [a,*], Aziz-ur-Rehman [b], Ismat Bibi [c,*], Najla AlMasoud [d], Taghrid S. Alomar [d], Munawar Iqbal [e,*]

[a] *Department of Biochemistry, Government College University, Faisalabad 38000, Pakistan*
[b] *Department of Chemistry, Government College University, Lahore 54000, Pakistan*
[c] *Institute of Chemistry, The Islamia University of Bahawalpur, 63000, Bahawalpur, Pakistan*
[d] *Department of Chemistry, College of Science, Princess Nourah bint Abdulrahman University, P.O. Box 84428, Riyadh 11671, Saudi Arabia*
[e] *Department of Chemistry, Division of Science and Technology, University of Education, Lahore, Pakistan*

Received 26 August 2022; accepted 22 January 2023
Available online 25 January 2023

KEYWORDS

1,2,4-triazole;
Piperidine;
Acetylcholinesterase inhibition;
α-glucosidase inhibition

Abstract A series of novel triazole analogs (10a-k) bearing piperidine were synthesized in an aprotic solvent on the most effective pharmacophore with acetylcholinesterase (AChE) and α-glucosidase inhibitory activity. Triazole analogs (10a-k) were obtained in excellent yields (75–90 %) and characterized by EI-MS, IR, ^{13}C NMR and ^{1}H NMR. The newly synthesized triazole analogs (10a-k) showed potent AChE inhibitory activity in the range of K_i = 0.0155 ± 1.25 μM to 0.557 ± 0.50 μM, IC_{50} = 0.031 ± 0.85 to 0.537 ± 0.76 μM than Eserine (0.04 ± 0.001 μM) having strong electron-withdrawing fluorine group on the pyridine ring was recorded as a most potent inhibitor of AChE while (%) inhibition against α-glucosidase was ranging between 52.36 ± 1.67 to 85.35 ± 1.39. The kinetic study predicted that triazole analogs (10a-k) followed the un-competitive and mixed type of inhibition against AChE. In silico molecular docking was performed at the active site of the AChE co-crystal structure (PDB ID:1NEN). The results of molecular docking corelate will with the experimental findings.

* Corresponding author.
E-mail addresses: shagufta_kamal@yahoo.com (S. Kamal), drismat@iub.edu.pk (I. Bibi), bosalvee@yahoo.com (M. Iqbal).
Peer review under responsibility of King Saud University.

Production and hosting by Elsevier

https://doi.org/10.1016/j.arabjc.2023.104626

1. Introduction

Alzheimer's disease (AD) is characterized by the presence of neurofibrillary tangles, and neuritic plaques, associated with neuronal loss leading to term memories disturbances and confusion (Türkeş et al., 2021; Li et al., 2023; Hao et al., 2023; Taslimi et al., 2020). Following the cholinergic hypothesis, a deficit in the level of acetylcholine (ACh) subsequently affecting intervening memory function results in memory reduction. AChE hydrolyzes the ACh released at cholinergic synapses into acetate and choline. This amelioration results in the depletion of Ach causing a diminution in the cognitive deficit (Güleç et al., 2017; Güleç et al., 2022). However, inhibition of AChE performs an essential role in cholinergic communication and takes part in different functions appertaining to adhesion, differentiation, and neuronal development (Avula et al., 2018). To date, there is no cure for AD (Bechara et al., 2015). However, AChE inhibitors were envisaged as remedies for AD treatment because they can reduce toxic amyloid β-peptide formation (Bechara et al., 2015). In short, AChE inhibitors (AChEIs) are responsible for improving the patient's quality of life thus leading to improved cognitive capability yet hampering the AD progression (Bousada et al., 2020). Literature reported that neurodegenerative AD and type-2 diabetes are interlinked (Türkeş et al., 2021). Interestingly, it is observed that AChE is associated with different complications and oxidative stress leading to the pathogenesis and progression of central neural disorders such as type-2 diabetes and AD (Taslimi et al., 2021).

Clinically, it is proven that diabetic patients are at higher risk of cognitive impairments and dementia (Türkeş et al., 2021). Therefore, inhibition of α-glycosidase would reduce the process of carbohydrate digestion and would preclude postprandial hyperglycemia which is a major consequence of diabetes complications (Akocak et al., 2021). In light of these pieces of information, it is understood that AChE and α-glucosidase inhibitors can treat both AD and DM. Therefore, the synthesis or the development of novel compounds having appropriate bioactive properties and chemical structures to interact with these enzymes is an urgent need (Gümüş et al., 2022) Hence, because of our interest to develop potent anti-AD and anti-MD agents, we presented a series of novel triazole analogs (10a-k) by combining two essential rings of piperidine with triazole.

The heterocyclic triazole analogs have been proven to be important drug candidates owing to their activity in different biological fields including material science, nano-chemistry, biology, medicine, and agriculture (Sacchetti et al., 2022; Guan et al., 2022; Gaspar et al., 2022; Dubovis et al., 2018). In the field of medicine, analogs of triazole have acted as active antiviral (Gülçin et al., 2016), antifungal (Haddad et al., 2015), anti-inflammatory, antibacterial, anticonvulsant and anticancer agents (Honka et al., 2018; Jha et al., 2010; Kousar et al., 2020; Laube, 2002).neurodegenerative disorders require a thought-provoking resolution because of the alarming situation being faced owing to the ineffectiveness of reported drugs. Previous studies have emphasized the bioactivity of heterocyclic analogs against a variety of enzymes and pathogens which have been addressed through new active multifunctional drug candidates to deal with the ineffectiveness of drugs (Li and Zhang, 2021). Piperidine being an active synthetic pharmaceutical drug contained alkaloids such as (S)-coniine, (S)-anabasine, (–)-swainsonine, and quinine (Sacchetti et al., 2022; Guan et al., 2022; Gaspar et al., 2022; Dubovis et al., 2018; Honka et al., 2018; Jha et al., 2010; Kousar et al., 2020; Laube, 2002).

Herein, complete synthesis, structural and molecular characterization along with AChE and α-glucosidase inhibitory effects are reported and tried to discover the most potent and favorable α-glucosidase and AChE inhibition properties of novel triazole analogs (10a-k) to stretch directions to further studies.

2. Experimental

2.1. Chemicals and instruments

All the experiments were carried out under aerobic conditions unless stated otherwise. Alfa Aesar, Sigma Aldrich and Merck were contacted for analytical grade chemicals and solvents through local suppliers and forwarded to reaction as such. Melting points of the synthesized compounds (Acetylcholinesterase and α-Glucosidase inhibitors) were computed through Griffin and George apparatus. IR spectral patterns were recorded by Jasco-320A spectrometer using the KBr disc method. FT NMR (^{1}H and ^{13}C) spectra of the synthesized compounds (**10a-k**) were collected by Bruker 600 MHz in deuterated dimethyl sulfoxide (DMSO d_6). JMS-HX-110 spectrometer was a tool for recording EI-MS spectra. The TLC plates were observed in UV light at 254 nm or iodine vapors and were made of aluminum plates pre-coated by silica gel.

2.2. Synthesis of 1-(4-toluenesulfonyl)-4-(ethoxycarbonyl) piperidine (3)

1,2,4 Trizole was synthesized by following the scheme-1 described by previously reported methods of (Bitla et al., 2021) 4-Ethoxycarbonylpiperidine (**2**; 0.05 mol) was mixed with 20 % $Na_2CO_{3(aq)}$ in 500 mL round bottom (RB) flask. 4-Toluenesulfonyl chloride (**1**; 0.05 mol) was added by parts on stirring $Na_2CO_{3(aq)}$ was used to maintain PH = 10 TLC was monitored to confirm completion. The pH of the medium was moved to 6 by dilute $HCl_{(aq)}$. The title compound was collected as precipitates, washed, and dried.

2.3. Synthesis of 1-(4-toluenesulfonyl)-4-(2-hydrazinocarbonyl) piperidine (5)

Hydrazine monohydrate (**4**; 0.045 mol) and equimolar compound **3** were shaken together in methanol (150 mL) in RB flask (500 mL). The contents of the flask were refluxed for 4 h and monitored through TLC. The precipitates were collected after distillation of methanol, washed with *n*-hexane and dried in air.

2.4. Synthesis of 1-(4-toluenesulfonyl)-4-[1-(methylamino thiocarbonyl)-2 hydrazinocarbonylpiperidine(7)

Equimolar compound **5** and methyl isothiocyanate (**6**) were shaken together in ethanol (150 mL) in RB flask (500 mL). The contents of the flask were refluxed for 2 h and monitored through TLC. The precipitates were collected after the distillation of the ethanol. Formed precipitates were washed through distilled water and dried in air.

2.5. Procedure for 1-(4-toluenesulfonyl)-4-(3-mercapto-4-methyl-4H-1,2,4-triazol-5-yl)piperidine (8)

Compound **7** (0.04 mol) was refluxed with 15 % $KOH_{(aq)}$ for 2 h and monitored through TLC. The pH of the medium was moved to 6 by dilute $HCl_{(aq)}$. The title compound was collected as precipitates, washed and dried.

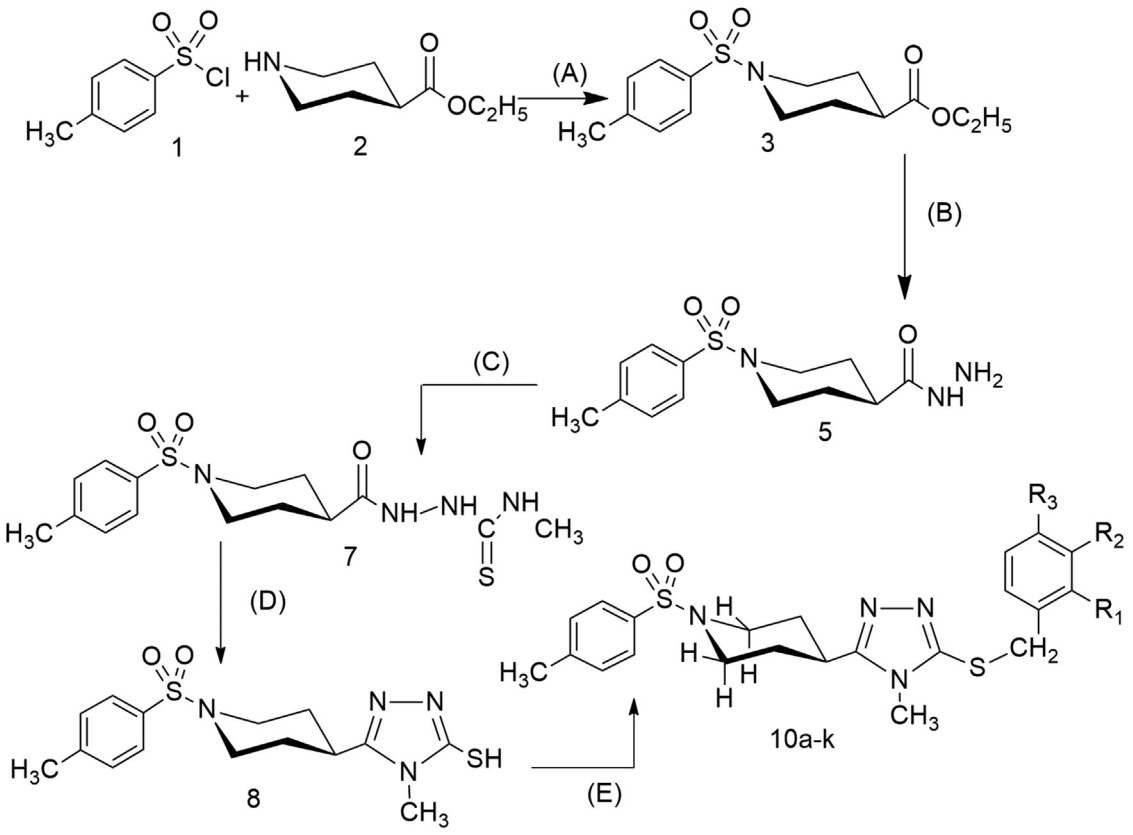

Comp	R_1	R_2	R_3	Comp	R_1	R_2	R_3
10a	H	H	H	10f	H	H	Cl
10b	Metyl	H	H	10g	Br	H	H
10c	H	Metyl	H	10h	H	Br	H
10d	H	H	Metyl	10i	H	H	Br
10e	Cl	H	H	10j	H	H	F
				10k	H	Cl	Cl

Scheme 1 Synthesis of 1-(4-toluenesulfonyl)-4-(3-aralkylthio-4-methyl-4*H*-1,2,4-triazol-5-yl) piperidine (**10a-k**). **Reagents and conditions:** (**A**) Stirring at RT with 20 % $Na_2CO_{3(aq)}$ and pH = 10 (**B**) Refluxing with $NH_2NH_2{\cdot}H_2O$ (**4**) in MeOH (**C**) Refluxing with CH_3NCS (**6**) in EtOH (**D**) Refluxing with 15 % $KOH_{(aq)}$ (**E**) Stirring at RT with LiH in DMF.

2.6. Procedure for 1-(4-toluenesulfonyl)-4-(3-aralkylthio-4-methyl-4H-1,2,4-triazol-5-yl)piperidine (10a-k)

Compound **8** (2 mmol) and LiH (2 mmol) were shaken together in DMF (15 mL) in RB flask (100 mL) and stirred for 0.5 h. Equimolar aralkyl halides (**9a-k**) were added and the contents of the flask were stirred for 3–5 h. TLC was performed and precipitates were collected after the addition of ice-cold distilled water. The title compounds were collected as precipitates, washed and dried.

2.7. 1-(4-Toluenesulfonyl)-4-(3-benzylthio-4-methyl-4H-1,2,4-triazol-5-yl)piperidine (10a)

Amorphous white solid;; M.P.: 186–188 °C; Yield: 86 %; IR (υ_{max}, cm^{-1}): 3061, 1670, 1548, 1367, 694;^{1}H NMR (600 MHz, DMSO d_6, δ ppm): 7.66 (2H, J = 7.6 Hz, d,2'' & 6''), 7.48 (2H, J = 7.6 Hz, d,3'' & 5''), 7.27–7.25 (3H, m, 3''' to 5'''), 7.22 (2H, J = 6.8 Hz, d,2''' & 6'''), 4.24 (2H, s, 7'''), 3.64–3.62 ($2H_e$, m, 2′ & 6′), 3.19 (3H, s, 6), 2.81–2.77 (1H, m, 4′), 2.42 (3H, s, 7''), 2.42–2.39 ($2H_a$, m, 2′ & 6′), 1.89–

1.87 ($2H_e$, m, 3′ & 5′), 1.74–1.68 ($2H_a$, m, 3′ & 5′);^{13}C NMR (125 MHz, DMSO d_6, δ ppm): 157.7 (5), 148.4 (3), 143.4 (1′′), 137.2 (1′′′), 132.3 (4′′), 129.8 (3′′ & 5′′), 128.8 (2′′′ & 6′′′), 128.3 (3′′′ & 5′′′), 127.5 (2′′ & 6′′), 127.3 (4′′′), 45.4 (2′ & 6′), 37.5 (4′), 30.4 (7′′′), 29.6 (6), 28.8 (3′ & 5′), 20.9 (7′′); M.F.: $C_{22}H_{26}N_4O_2S_2$; M.W.: 442 gmol^{-1}; EI-MS (*m*/*z*): 442 $[M]^+$, 319 $[C_{15}H_{19}N_4O_2S]^+$, 293 $[C_{14}H_{19}N_3O_2S]^{\cdot+}$, 287 $[C_{15}H_{19}N_4S]^+$, 264 $[C_{13}H_{16}N_2O_2S]^+$, 204 $[C_{10}H_{10}N_3S]^+$, 155 $[C_7H_7O_2S]^+$, 149 $[C_8H_7NS]^+$, 91 $[C_7H_7]^+$, 65 $[C_5H_5]^+$.

2.8. 1-(4-Toluenesulfonyl)-4-[3-(2-methylbenzyl) thio-4-methyl-4H-1,2,4-triazol-5-yl]piperidine (10b

Amorphous white solid;; M.P.: 178–180 °C; Yield: 88 %;; IR (υ_{max}, cm^{-1}): 3069, 1656, 1577, 1374, 689;^{1}H NMR (600 MHz, DMSO d_6, δ ppm): 7.65 (2H, *J* = 7.6 Hz, d, 2′′ & 6′′), 7.46 (2H, *J* = 7.5 Hz, d, 3′′ & 5′′), 7.02–6.95 (4H, m,3′′′ to 6′′′), 4.19 (2H, s, 7′′′), 3.63–3.61 ($2H_e$, m, 2′ & 6′), 3.20 (3H, s, 6), 2.80 (1H, br.s, 4′), 2.42 (3H, s, 7′′), 2.42–2.40 ($2H_a$,m, 2′ & 6′), 2.24 (3H, s, 8′′′), 1.89–1.85 ($2H_e$, m, 3′ & 5′), 1.74–1.69 ($2H_a$, m, 3′ & 5′);^{13}C NMR (125 MHz, DMSO d_6, δ ppm): 157.6 (5), 148.6 (3), 143.4 (1′′), 137.8 (1′′′), 132.3 (4′′), 131.4 (2′′′), 130.2 (3′′′), 129.8 (3′′ & 5′′), 128.3 (4′′′), 127.9 (6′′′),127.5 (2′′ & 6′′), 127.3 (5′′′), 45.4 (2′ & 6′), 37.4 (4′), 30.4 (7′′′), 29.5 (6), 28.8 (3′ & 5′), 20.9 (7′′), 20.6 (8′′′); M.F.: $C_{23}H_{28}N_4O_2S_2$; M.W.: 456 gmol^{-1}. EI-MS (*m*/*z*): 456 $[M]^+$, 319 $[C_{15}H_{19}N_4O_2S]^+$, 301 $[C_{16}H_{21}N_4S]^+$, 293 $[C_{14}H_{19}N_3O_2S]^{\cdot+}$, 264 $[C_{13}H_{16}N_2O_2S]^+$, 218 $[C_{11}H_{12}N_3S]^+$, 163 $[C_9H_9NS]^+$, 155 $[C_7H_7O_2S]^+$, 105 $[C_8H_9]^+$, 65 $[C_5H_5]^+$.

2.9. 1-(4-Toluenesulfonyl)-4-[3-(3-methylbenzyl)thio-4-methyl-4H-1,2,4-triazol-5-yl]piperidine (10c)

Amorphous white solid; M.P.: 170–172 °C; Yield: 79 %;;IR (υ_{max}, cm^{-1}):3063, 1659, 1570, 1371, 682;^{1}H NMR (600 MHz, DMSO d_6, δ ppm): 7.65 (2H, *J* = 7.3 Hz, d, 2′′ & 6′′), 7.47 (2H, *J* = 7.5 Hz, d, 3′′ & 5′′), 7.15 (1H, *J* = 7.4 Hz, t, 5′′′), 7.06 (1H, *J* = 7.4 Hz, d, 6′′′), 7.01 (1H, s, 2′′′), 7.01–6.99 (1H, m, 4′′′), 4.18 (2H, s, 7′′′), 3.63–3.62 ($2H_e$, m, 2′ & 6′), 3.19 (3H, s, 6), 2.79 (1H, br.s, 4′), 2.41 (3H, s, 7′′), 2.41–2.39 ($2H_a$, m, 2′ & 6′), 2.23 (3H, s, 8′′′), 1.89–1.86 ($2H_e$, m, 3′ & 5′), 1.73–1.69 ($2H_a$, m, 3′ & 5′);^{13}C NMR (125 MHz, DMSO d_6, δ ppm): 157.7 (5), 148.5 (3), 143.4 (1′′), 137.5 (1′′′), 137.0 (3′′′), 132.3 (4′′), 129.8 (3′′ & 5′′), 129.3 (5′′′), 128.3 (4′′′), 128.0 (2′′′), 127.5 (2′′ & 6′′), 125.9 (6′′′), 45.4 (2′ & 6′), 37.6 (4′), 30.4 (7′′′), 29.5 (6), 28.8 (3′ & 5′), 20.9 (7′′), 20.8 (8′′′); M.F.: $C_{23}H_{28}N_4O_2S_2$; M.W.: 456 gmol^{-1}. EI-MS (*m*/*z*): 456 $[M]^+$, 319 $[C_{15}H_{19}N_4O_2S]^+$, 301 $[C_{16}H_{21}N_4S]^+$, 293 $[C_{14}H_{19}N_3O_2S]^{\cdot+}$, 264 $[C_{13}H_{16}N_2O_2S]^+$, 218 $[C_{11}H_{12}N_3S]^+$, 163 $[C_9H_9NS]^+$, 155 $[C_7H_7O_2S]^+$, 105 $[C_8H_9]^+$, 65 $[C_5H_5]^+$.

2.10. 1-(4-Toluenesulfonyl)-4-[3-(4-methylbenzyl) thio-4-methyl-4H-1,2,4-triazol-5-yl]piperidine (10d)

Amorphous white solid; M.P.: 186–188 °C; Yield: 87 %; IR (υ_{max}, cm^{-1}):3073, 1659, 1580, 1382, 687;^{1}H NMR (600 MHz, DMSO d_6, δ ppm): 7.65 (2H, *J* = 7.4 Hz, d, 2′′ & 6′′), 7.47 (2H, *J* = 7.5 Hz, d, 3′′ & 5′′), 7.10 (2H, *J* = 7.4 Hz, d, 2′′′ & 6′′′), 7.07 (2H, *J* = 7.4 Hz, d, 3′′′ & 5′′′), 4.19 (2H, s, 7′′′), 3.63–3.62 ($2H_e$, m, 2′ & 6′), 3.20 (3H, s, 6), 2.79 (1H, br.s, 4′), 2.41 (3H, s, 7′′), 2.41–2.39 ($2H_a$, m, 2′ & 6′), 2.25 (3H, s, 8′′′), 1.89–1.86 ($2H_e$, m, 3′ & 5′), 1.71–1.69 ($2H_a$, m, 3′ & 5′);^{13}C NMR (125 MHz, DMSO d_6, δ ppm): 157.7 (5), 148.5 (3), 143.4 (1′′), 136.6 (1′′′), 134.0 (4′′′), 132.3 (4′′), 129.8 (3′′ & 5′′), 128.9 (3′′′ & 5′′′), 128.7 (2′′′ & 6′′′), 127.5 (2′′ & 6′′), 45.4 (2′ & 6′), 37.2 (4′), 30.4 (7′′′), 29.5 (6), 28.8 (3′ & 5′), 20.9 (7′′), 20.6 (8′′′); M.F.: $C_{23}H_{28}N_4O_2S_2$; M.W.: 456 gmol^{-1}; EI-MS (*m*/*z*): 456 $[M]^+$, 319 $[C_{15}H_{19}N_4O_2S]^+$, 301 $[C_{16}H_{21}N_4S]^+$, 293 $[C_{14}H_{19}N_3O_2S]^{\cdot+}$, 264 $[C_{13}H_{16}N_2O_2S]^+$, 218 $[C_{11}H_{12}N_3S]^+$, 163 $[C_9H_9NS]^+$, 155 $[C_7H_7O_2S]^+$, 105 $[C_8H_9]^+$, 65 $[C_5H_5]^+$.

2.11. 1-(4-Toluenesulfonyl)-4-[3-(2-chlorobenzyl)thio-4-methyl-4H-1,2,4-triazol-5-yl]piperidine (10e)

Amorphous white solid; M.P.: 168–170 °C; Yield: 83 %;;IR (υ_{max}, cm^{-1}):3087, 1666, 1589, 1396, 702, 691;^{1}H NMR (600 MHz, DMSO d_6, δ ppm): 7.66 (2H, *J* = 8.1 Hz, d, 2′′ & 6′′), 7.47 (2H, *J* = 8.0 Hz, d, 3′′ & 5′′), 7.44 (1H, *J* = 7.9 Hz, d, 6′′′), 7.30 (1H, *J* = 2.9, 6.2 Hz, dt, 4′′′), 7.24–7.22 (2H, m, 3′′′ & 5′′′), 4.29 (2H, s, 7′′′), 3.65–3.63 ($2H_e$, m, 2′ & 6′), 3.36 (3H, s, 6), 2.82–2.78 (1H, m, 4′), 2.42 (3H, s, 7′′), 2.42–2.40 ($2H_a$, m, 2′ & 6′), 1.89–1.87 ($2H_e$, m, 3′ & 5′), 1.75–1.68 ($2H_a$, m, 3′ & 5′);^{13}C NMR (125 MHz, DMSO d_6, δ ppm): 158.0 (5), 147.8 (3), 143.4 (1′′), 134.6 (1′′′), 133.0 (5′′′), 132.3 (4′′), 131.2 (3′′′), 129.7 (3′′ & 5′′), 129.5 (4′′′), 129.4 (6′′′), 127.5 (2′′ & 6′′), 127.2 (2′′′), 45.4 (2′ & 6′), 35.7 (4′), 30.5 (7′′′), 29.5 (6), 28.8 (3′ & 5′), 20.9 (7′′); M.F.: $C_{22}H_{25}ClN_4O_2S_2$; M.W.: 477 gmol^{-1} EI-MS (*m*/*z*): 479 $[M + 2]^+$, 477 $[M]^+$, 321 $[C_{15}H_{18}ClN_4S]^+$, 319 $[C_{15}H_{19}N_4O_2S]^+$, 293 $[C_{14}H_{19}N_3O_2S]^{\cdot+}$, 264 $[C_{13}H_{16}N_2O_2S]^+$, 238 $[C_{10}H_9ClN_3S]^+$, 183 $[C_8H_6ClNS]^+$, 155 $[C_7H_7O_2S]^+$, 125 $[C_7H_6Cl]^+$, 65 $[C_5H_5]^+$.

2.12. 1-(4-Toluenesulfonyl)-4-[3-(4-chlorobenzyl) thio-4-methyl-4H-1,2,4-triazol-5-yl]piperidine (10f)

Amorphous white solid; M.P.: 174–176 °C; Yield: 90 %; IR (υ_{max}, cm^{-1}):3081, 1660, 1584, 1399, 705, 688;^{1}H NMR (600 MHz, DMSO d_6, δ ppm): 7.66 (2H, *J* = 7.5 Hz, d, 2′′ & 6′′), 7.48 (2H, *J* = 7.6 Hz, d, 3′′ & 5′′), 7.34 (2H, *J* = 7.9 Hz, d, 2′′′ & 6′′′), 7.27 (2H, *J* = 7.4 Hz, d, 3′′′ & 5′′′), 4.25 (2H, s, 7′′′), 3.64–3.62 ($2H_e$, m, 2′ & 6′), 3.26 (3H, s, 6), 2.81 (1H, br.s, 4′), 2.42 (3H, s, 7′′), 2.42–2.39 ($2H_a$, m, 2′ & 6′), 1.90–1.87 ($2H_e$, m, 3′ & 5′), 1.73–1.69 ($2H_a$, m, 3′ & 5′);^{13}C NMR (125 MHz, DMSO d_6, δ ppm): 157.8 (5), 148.2 (3), 143.4 (1′′), 136.4 (4′′′), 132.3 (4′′), 131.9 (1′′′), 130.7 (3′′′ & 5′′′), 129.8 (3′′ & 5′′), 128.3 (2′′′ & 6′′′), 127.5 (2′′ & 6′′), 45.4 (2′ & 6′), 36.4 (4′), 30.4 (7′′′), 29.6 (6), 28.8 (3′ & 5′), 20.9 (7′′); M.F.: $C_{22}H_{25}ClN_4O_2S_2$; M.W.: 477 gmol^{-1}; EI-MS (*m*/*z*): 479 $[M + 2]^+$, 477 $[M]^+$, 321 $[C_{15}H_{18}ClN_4S]^+$, 319 $[C_{15}H_{19}N_4O_2S]^+$, 293 $[C_{14}H_{19}N_3O_2S]^{\cdot+}$, 264 $[C_{13}H_{16}N_2O_2S]^+$, 238 $[C_{10}H_9ClN_3S]^+$, 183 $[C_8H_6ClNS]^+$, 155 $[C_7H_7O_2S]^+$, 125 $[C_7H_6Cl]^+$, 65 $[C_5H_5]^+$.

2.13. 1-(4-Toluenesulfonyl)-4-[3-(2-bromobenzyl) thio-4-methyl-4H-1,2,4-triazol-5-yl] piperidine (10 g)

Amorphous white solid; M.P.: 178–180 °C; Yield: 75 %; IR (υ_{max}, cm^{-1}):3098, 1673, 1591, 1394, 653, 682;^{1}H NMR

(600 MHz, DMSO d_6, δ ppm): 7.65 (2H, J = 8.0 Hz, d, 2'' & 6''), 7.61 (1H, J = 7.7 Hz, d, 6'''), 7.46 (2H, J = 8.1 Hz, d, 3'' & 5''), 7.32 (1H, J = 7.2 Hz, t, 4'''), 7.26 (1H, J = 6.9 Hz, t, 5'''), 6.91 (1H, J = 7.6 Hz, d, 3'''), 4.29 (2H, s, 7'''), 3.65–3.61 ($2H_e$, m, 2′ & 6′), 3.20 (3H, s, 6), 2.79 (1H, br.s, 4′), 2.42 (3H, s, 7''), 2.42–2.41 ($2H_a$, m, 2′ & 6′), 1.90–1.87 ($2H_e$, m, 3′ & 5′), 1.74–1.71 ($2H_a$, m, 3′ & 5′);^{13}C NMR (125 MHz, DMSO d_6, δ,ppm): 158.0 (5), 147.8 (3), 143.4 (1''), 136.2 (1'''), 132.3 (4''), 131.2 (3'''), 129.8 (3'' & 5''), 129.5 (4'''), 128.6 (6'''), 127.8 (5'''), 127.5 (2'' & 6''), 121.9 (2'''), 45.4 (2′ & 6′), 38.2 (4′), 30.5 (7'''), 29.5 (6), 28.8 (3′ & 5′), 20.9 (7''); M.F.: $C_{22}H_{25}BrN_4O_2S_2$; M.W.: 521 gmol^{-1}; EI-MS (m/z): 523 $[M + 2]^+$, 521 $[M]^+$, 366 $[C_{15}H_{18}BrN_4S]^+$, 319 $[C_{15}H_{19}N_4O_2S]^+$, 293 $[C_{14}H_{19}N_3O_2S]^{\cdot+}$, 283 $[C_{10}H_9BrN_3S]^+$, 264 $[C_{13}H_{16}N_2O_2S]^+$, 228 $[C_8H_6BrNS]^+$, 170 $[C_7H_6Br]^+$, 155 $[C_7H_7O_2S]^+$, 65 $[C_5H_5]^+$.

2.14. 1-(4-Toluenesulfonyl)-4-[3-(3-bromobenzyl)thio-4-methyl-4H-1,2,4-triazol-5-yl] piperidine (10 h)

Amorphous white solid; M.P.: 172–174 °C; Yield: 79 %;; IR (υ_{max}, cm^{-1}):3086, 1681, 1595, 1391, 649, 688;^{1}H NMR (600 MHz, DMSO d_6, δ ppm): 7.65 (2H, J = 7.6 Hz, d, 2'' & 6''), 7.47 (2H, J = 7.5 Hz, d, 3'' & 5''), 7.33 (1H, s, 2'''), 7.17–7.13 (2H, m, 5''' & 6'''), 6.97 (1H, J = 7.5 Hz, d, 4'''), 4.25 (2H, s, 7'''), 3.63–3.61 ($2H_e$, m, 2′ & 6′), 3.20 (3H, s, 6), 2.79 (1H, br.s, 4′), 2.41 (3H, s, 7''), 2.41–2.39 ($2H_a$, m, 2′ & 6′), 1.89–1.85 ($2H_e$, m, 3′ & 5′), 1.74–1.68 ($2H_a$, m, 3′ & 5′);^{13}C NMR (125 MHz, DMSO d_6, δ ppm): 157.9 (5), 148.2 (3), 143.4 (1''), 140.2 (1'''), 132.3 (4''), 131.4 (4'''), 130.4 (2'''), 130.1 (5'''), 129.8 (3'' & 5''), 127.9 (6'''), 127.5 (2'' & 6''), 121.3 (3'''), 45.4 (2′ & 6′), 36.5 (4′), 30.4 (7'''), 29.5 (6), 28.8 (3′ & 5′), 20.9 (7''); M.F.: $C_{22}H_{25}BrN_4O_2S_2$; M.W.: 521 gmol^{-1} EI-MS (m/z): 523 $[M + 2]^+$, 521 $[M]^+$, 366 $[C_{15}H_{18}BrN_4S]^+$, 319 $[C_{15}H_{19}N_4O_2S]^+$, 293 $[C_{14}H_{19}N_3O_2S]^{\cdot+}$, 283 $[C_{10}H_9BrN_3S]^+$, 264 $[C_{13}H_{16}N_2O_2S]^+$, 228 $[C_8H_6BrNS]^+$, 170 $[C_7H_6Br]^+$, 155 $[C_7H_7O_2S]^+$, 65 $[C_5H_5]^+$.

2.15. 1-(4-Toluenesulfonyl)-4-[3-(4-bromobenzyl)thio-4-methyl-4H-1,2,4-triazol-5-yl] piperidine (10i)

Amorphous white solid; M.P.: 182–184 °C; Yield: 75 %; IR (υ_{max}, cm^{-1}):3076, 1679, 1597, 1388, 647, 685;^{1}H NMR (600 MHz, DMSO d_6, δ ppm): 7.65 (2H, J = 7.3 Hz, d, 2'' & 6''), 7.48–7.46 (4H, m, 4H, 3'' & 5'', 2''' & 6'''), 7.20 (2H, J = 7.2 Hz, d, 3''' & 5'''), 4.23 (2H, s, 7'''), 3.64–3.62 ($2H_e$, m, 2′ & 6′), 3.26 (3H, s, 6), 2.82–2.79 (1H, m, 4′), 2.42 (3H, s, 7''), 2.42–2.40 ($2H_a$, m, 2′ & 6′), 1.90–1.88 ($2H_e$, m, 3′ & 5′), 1.74–1.68 ($2H_a$, m, 3′ & 5′);^{13}C NMR (125 MHz, DMSO d_6, δ ppm): 157.8 (5), 148.2 (3), 143.4 (1''), 136.8 (1'''), 132.3 (4''), 131.2 (3''' & 5'''), 131.0 (2''' & 6'''), 129.8 (3'' & 5''), 127.5 (2'' & 6''), 120.5 (4'''), 45.4 (2′ & 6′), 36.4 (4′), 30.4 (7'''), 29.6 (6), 28.8 (3′ & 5′), 20.9 (7''); M.F.: $C_{22}H_{25}BrN_4O_2S_2$; M.W.: 521 gmol^{-1}; EI-MS (m/z): 523 $[M + 2]^+$, 521 $[M]^+$, 366 $[C_{15}H_{18}BrN_4S]^+$, 319 $[C_{15}H_{19}N_4O_2S]^+$, 293 $[C_{14}H_{19}N_3O_2S]^{\cdot+}$, 283 $[C_{10}H_9BrN_3S]^+$, 264 $[C_{13}H_{16}N_2O_2S]^+$, 228 $[C_8H_6BrNS]^+$, 170 $[C_7H_6Br]^+$, 155 $[C_7H_7O_2S]^+$, 65 $[C_5H_5]^+$.

2.16. 1-(4-Toluenesulfonyl)-4-[3-(4-flourobenzyl) thio-4-methyl-4H-1,2,4-triazol-5-yl]piperidine (10j)

Amorphous white solid; M.P.: 170–172 °C; Yield: 81 %; IR (υ_{max}, cm^{-1}):3096, 1669, 1584, 1389, 1057, 676;^{1}H NMR (600 MHz, DMSO d_6, δ ppm): 7.65 (2H, J = 7.6 Hz, d, 2'' & 6''), 7.45 (2H, J = 7.6 Hz, d, 3'' & 5''), 7.21 (2H, J = 8.1 Hz, d, 3''' & 5'''), 7.02 (2H, J = 8.0 Hz, d, 2''' & 6'''), 4.24 (2H, s, 7'''), 3.64–3.61 ($2H_e$, m, 2′ & 6′), 3.21 (3H, s, 6), 2.80 (1H, br.s, 4′), 2.42 (3H, s, 7''), 2.42–2.39 ($2H_a$, m, 2′ & 6′), 1.90–1.88 ($2H_e$, m, 3′ & 5′), 1.72–1.69 ($2H_a$, m, 3′ & 5′);^{13}C NMR (600 MHz, DMSO d_6, δ ppm): 158.1 (5), 150.5 (4'''), 148.1 (3), 143.4 (1''), 132.1 (4''), 131.8 (1'''), 130.6 (2''' & 6'''), 129.8 (3'' & 5''), 127.5 (2'' & 6''), 127.1 (3''' & 5'''), 45.4 (2′ & 6′), 36.4 (4′), 30.4 (7'''), 29.6 (6), 28.8 (3′ & 5′), 20.9 (7''); M.F.: $C_{22}H_{25}FN_4O_2S_2$; M.W.: 460 gmol^{-1}; EI-MS (m/z): 460 $[M]^+$, 319 $[C_{15}H_{19}N_4O_2S]^+$, 305 $[C_{15}H_{18}FN_4S]^+$, 293 $[C_{14}H_{19}N_3O_2S]^{\cdot+}$, 264 $[C_{13}H_{16}N_2O_2S]^+$, 222 $[C_{10}H_9FN_3S]^+$, 167 $[C_8H_6FNS]^+$, 155 $[C_7H_7O_2S]^+$, 109 $[C_7H_6F]^+$, 65 $[C_5H_5]^+$.

2.17. 1-(4-Toluenesulfonyl)-4-[3-(3,4-dichlorobenzyl)thio-4-methyl-4H-1,2,4-triazol-5-yl] piperidine (10 k)

Amorphous white solid; M.P.: 176–178 °C; Yield: 78 %; IR (υ_{max}, cm^{-1}):3066, 1658, 1579, 1388, 707, 686;^{1}H NMR (600 MHz, DMSO d_6, δ ppm): 7.66 (2H, J = 7.4 Hz, d, 2'' & 6''), 7.59 (1H, s, 2'''), 7.47 (2H, J = 7.5 Hz, d, 3'' & 5''), 7.33 (1H, J = 8.3 Hz, t, 5'''), 7.30 (1H, J = 8.0 Hz, d, 6'''), 4.28 (2H, s, 7'''), 3.65–3.63 ($2H_e$, m, 2′ & 6′), 3.28 (3H, s, 6), 2.84–2.80 (1H, m, 4′), 2.42 (3H, s, 7''), 2.42–2.40 ($2H_a$, m, 2′ & 6′), 1.90–1.88 ($2H_e$, m, 3′ & 5′), 1.75–1.69 ($2H_a$, m, 3′ & 5′);^{13}C NMR (600 MHz, DMSO d_6, δ ppm): 158.0 (5), 147.6 (3), 143.4 (1''), 133.99 (1'''), 133.94 (4'''), 133.0 (3'''), 132.4 (5'''), 132.3 (4''), 129.7 (3'' & 5''), 128.8 (2'''), 127.5 (2'' & 6''), 127.3 (6'''), 45.4 (2′ & 6′), 34.7 (4′), 30.5 (7'''), 29.6 (6), 28.8 (3′ & 5′), 20.9 (7''); M.F.: $C_{22}H_{24}Cl_2N_4O_2S_2$; M.W.: 511 gmol^{-1}; EI-MS (m/z): 515 $[M + 4]^+$, 513 $[M + 2]^+$, 511 $[M]^+$, 356 $[C_{15}H_{17}Cl_2N_4S]^+$, 319 $[C_{15}H_{19}N_4O_2S]^+$, 293 $[C_{14}H_{19}N_3O_2S]^{\cdot+}$, 273 $[C_{10}H_8Cl_2N_3S]^+$, 264 $[C_{13}H_{16}N_2O_2S]^+$, 218 $[C_8H_5Cl_2NS]^+$, 160 $[C_7H_5Cl_2]^+$, 155 $[C_7H_7O_2S]^+$, 65 $[C_5H_5]^+$.

2.18. In-vitro acetylcholinesterase (AChE) inhibition assay

Acetylcholinesterase (3.1.1.7) inhibition activity was measured by modifying the reported methods of Ellman using 96-wells plate readers (Synergy HT, BioTek, USA) (Mitsumori et al., 2003). Acetylcholine Iodide (AChEI) was used as the substrate, 5,5′-dithio bis (2-nitro benzoic) acid (DTNB) to estimate the activity of AChE and Eserine as reference. The reaction mixture containing 10 μL cholinesterase enzyme (Sigma, USA), tested compounds (0.05 mM; 10 to 100 mM), 60 μL phosphate buffer (pH 7.7; 0.05 mM), and 10 μL DTNB (0.05 mM) was incubated at 37 °C for 15–30 min. The change in optical density (O.D.) at zero, 15, and 30 min was monitored at 405 nm after the initiation of the reaction by the addition of

acetyl thiocholine iodide (10 µL) while Eserine (0.5 mM) was employed as a positive control. The percentage inhibition was noted as,

$$\textbf{Inhibition}(\%) = \frac{\textbf{Control} - \textbf{Test}}{\textbf{Control}} \times 100$$

The Ez-Fit software (Perrella Scientific Inc. Amherst, USA) and computing data in Graph Pad Prism 5 software were used to calculate IC_{50} values. Inhibition parameters and Vmax were determined from Lineweaver-Burk plots (Duyckaerts et al., 2009).

2.19. In-vitro α-Glucosidase assay

α-Glucosidase inhibition assay was performed following the reported methods of with minor modifications using acarbose as a reference standard (Tao et al., 2013). Tested compounds (10 to 100 µL; 0.05 mM), α-glucosidase enzyme (10 µL) (Sigma, USA) and phosphate buffers (70 µL; pH 6.8; 0.05 M) were mixed and pre-incubated at 37 °C for 10 min followed by pre-reading at 400 nm. Change in absorbance was monitored by adding *p*-nitrophenyl glucopyranoside (10 µL; 0.5 mM). The previously mentioned formula was used to assess the % inhibition and IC_{50} values.

2.20. Molecular docking simulations

The inhibitory potential of produced compounds was determined theoretically by virtual molecular docking software by Molegro Virtual Docker version 2010. Proteins for anti-acetylcholine esterase were saved as pdb after downloading from an online protein data bank. Chemdarw (Pro; 12.0.2; 875–317589-4732; Cambridgesoft) was used to draw the structures of produced compounds (10a-k) and saved as a MOL2 file by copying it into 3D chem draw. Files of pdb proteins were imported in the docking software to prepare a template then all produced compounds were run one by one.

3. Results and discussion

The target compounds 1,2,4-triazole analogs (**10a-k)** bearing piperidine were prepared under multiple-step synthesis presented having different functional groups depicted in Scheme 1. The main core of the 1,2,4-triazole nucleus (**8**) was achieved through the formation of different intermediates including carboxylate (**3**), hydrazide (**5**), and thiosemicarbazide (**7**). The last step resulted in 1,2,4-triazole analogs (**10a-k)**. Similar to our findings, (Castaneda et al., 2010)also reported the synthesis of 1,3,5 substituted 1,2,4 triazole from carboxylic acid but with only 25–84 % yield. Furthermore, two enzymes including acetylcholinesterase (AChE) and α-glucosidase were employed to demonstrate the enzyme inhibition potential of synthesized compounds (**10a-k**).

3.1. Chemistry

The compound **10d** has been explicated as a single compound discussion from this alkyl halide series (**10a-k**). The compounds, **10a-c**,**e-k**, have been structurally elucidated similarly. The white amorphous solid, **10d** ($C_{23}H_{28}N_4O_2S_2$, 456 g mol^{-1}, justified through mass spectrum), possessed a melting point of 186–188 °C with 87 % yield. The IR data was known to possess the following stretching frequencies for prominent functionalities, 3073, 1659, 1580, 1382 and 687. 4-Methylphenylsulfonyl moiety was justified through three signals in the ^{1}H NMR spectrum (Figs. 1, 2) at δ 7.65 (2H, *J* = 7.4 Hz, d, 2′’ & 6′’), 7.47 (2H, *J* = 7.5 Hz, d, 3′’ & 5′’) and 2.41 (3H, s, 7′’); and five signals in the ^{13}C NMR spectrum at δ 143.4 (1′’), 132.3 (4′’), 129.8 (3′’ & 5′’), 127.5 (2′’ & 6′’) and 20.9 (7′’). 4-Methylbenzyl moiety was justified through four signals in ^{1}H NMR spectrum (Figs. 1, 3) at δ 7.10 (2H, *J* = 7.4 Hz, d, 2′’’ & 6′’’), 7.07 (2H, *J* = 7.4 Hz, d, 3′’’ & 5′’’), 4.19 (2H, s, 7′’’) and 2.25 (3H, s, 8′’’); and six signals in ^{13}C NMR spectrum (Figure-4, Figure-5) at δ 136.6 (1′’’), 134.0 (4′’’), 128.9 (3′’’ & 5′’’), 128.7 (2′’’ & 6′’’), 30.4 (7′’’) and 20.6 (8′’’). 3,5-Disubstituted-6-methyl-1,2,4-triazole moiety was justified through one signal in the ^{1}H NMR spectrum (Fig. 2) at δ 3.20 (3H, s, 6); and three signals in the ^{13}C NMR spectrum (Figs. 4, 5) at δ 157.7 (5), 148.5 (3) and 29.5 (6). Piperidine moiety was justified through five signals in the ^{1}H NMR spectrum (Fig. 2) at δ 3.63–3.62 ($2H_e$, m, 2′ & 6′), 2.79 (1H, br.s, 4′), 2.41–2.39 ($2H_a$, m, 2′ & 6′), 1.89–1.86 ($2H_e$, m, 3′ & 5′) and 1.71–1.69 ($2H_a$, m, 3′ & 5′); and three signals in the ^{13}C NMR spectrum (Fig. 5) at δ 45.4 (2′ & 6′), 37.2 (4′) and 28.8 (3′ & 5′).

3.2. Biological activities

The biological activities of the prepared compounds were evaluated, which are important for practical applications (Muhammad et al., 2020; Suhail and Ali, 2020; Asif and Abida, 2019; Deeba et al., 2018; Pathak et al., 2021). The 1,2,4-triazole analogs (**10a-k)** were further evaluated for their inhibitory activities against AChE and α-glucosidase enzymes (Table 1, 2). It is investigated that AD and DM have an elevated activity of AChE (E.C. 3.1.1.7) which leads to alteration in cholinergic neurotransmission (Gulçin et al., 2018). Any alteration in the expression and activity of AChE that's a prime cause of neurodegenerative disorders may act as a biomarker for neurotoxicity determination (Isik et al., 2015) Inhibitors of AChE are widely recommended to eliminate neurotoxic effects produced by the change of the cholinergic hypothesis. Inhibitors of AChE may reduce the multiple β-amyloid neurotoxic products and protects the cell from oxidative damage (Taslimi et al., 2021). AChE inhibitors commonly used in treatment slow down excessive ACh hydrolysis and avert AD progression which leads to relaxation and improves cognitive functions (Isik et al., 2019)The structure–activity relationship (SAR) analysis revealed that the presence of electron-donating or electron-withdrawing groups at meta, ortho, or para positions of the whole series of derivatives (1,2,4-triazole analogs **10**a-k) presented a vital role in enhancing their anti-enzymatic role against AChE. The whole series of derivatives (1,2,4-triazole analogs **10**a-k) were active against the AChE enzyme (Table 1, 2, Figs. 6a & 6b). The excellent activity was possessed by four compounds, **10b** (bearing 2-methyl benzyl moiety), **10c** (bearing 3-methylbenzyl moiety), **10j** (bearing 4-fluorobenzyl moiety), and **10 k** (bearing 3,4-dichlorobenzyl moiety). among methyl-benzyl substituents, the most active ones were *ortho* and *meta*-substituted molecules, *ortho* substituted in the chlorobenzyl substituents, *meta* substituted in the bromobenzyl substituents, while *ortho* and

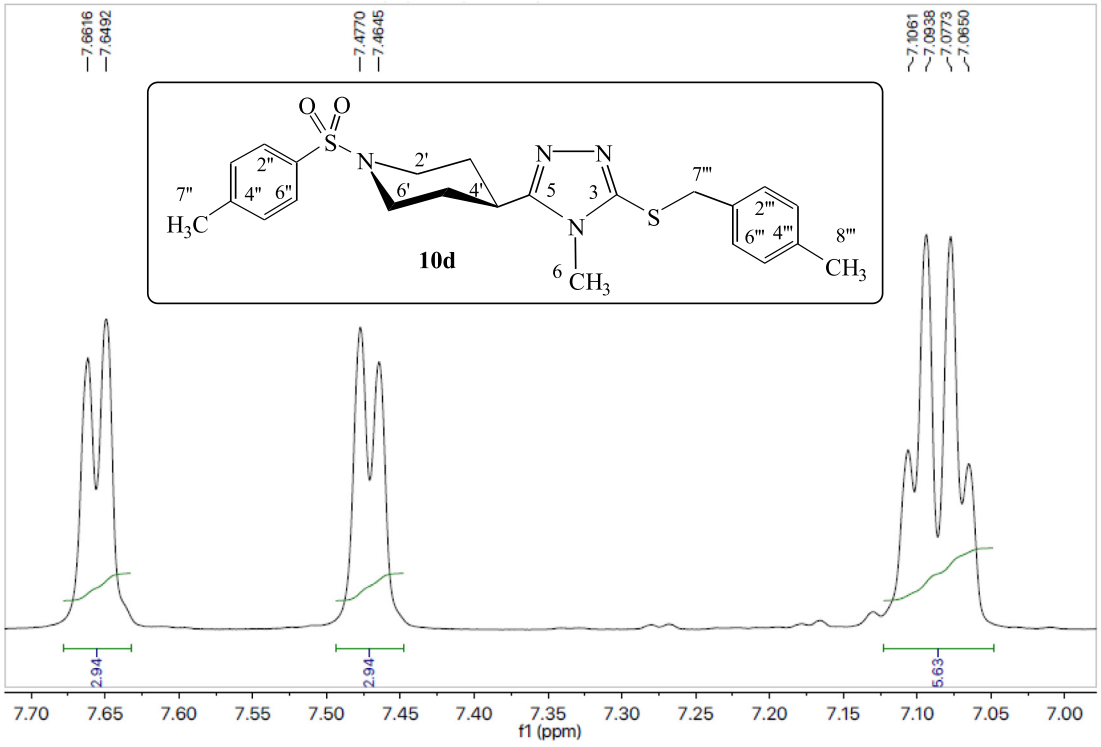

Fig. 1 ^{1}H NMR spectrum (aromatic) of compound **10d.**

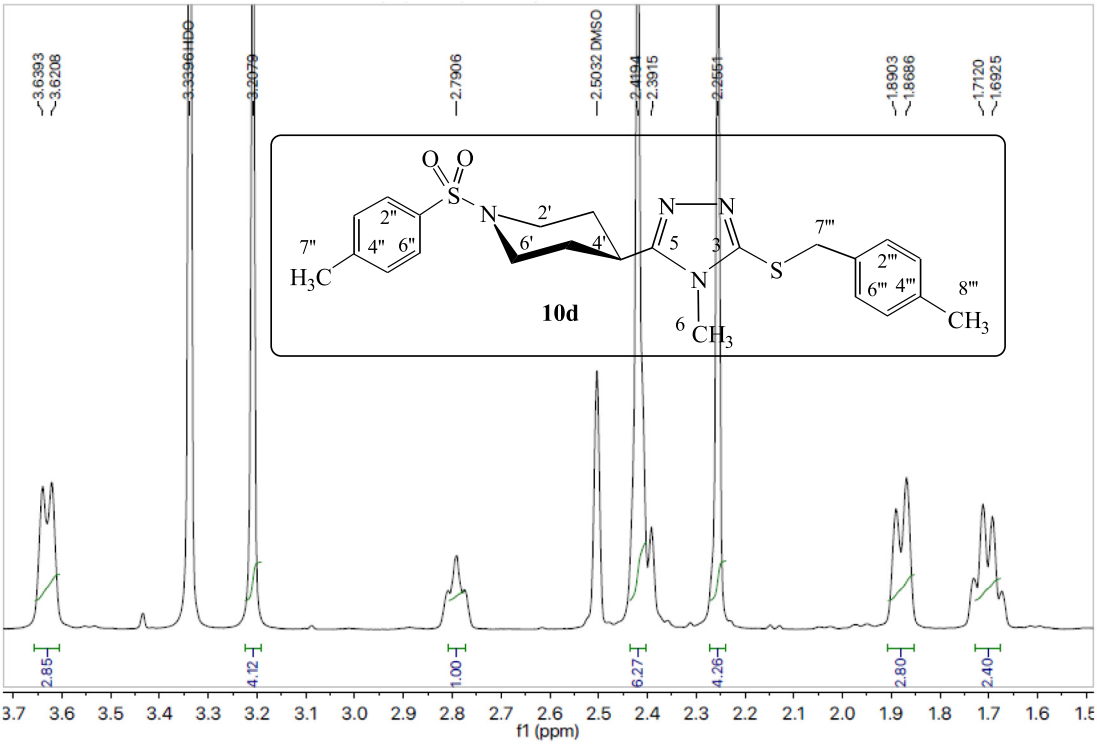

Fig. 2 ^{1}H NMR spectrum (shielded aliphatic) of compound **10d.**

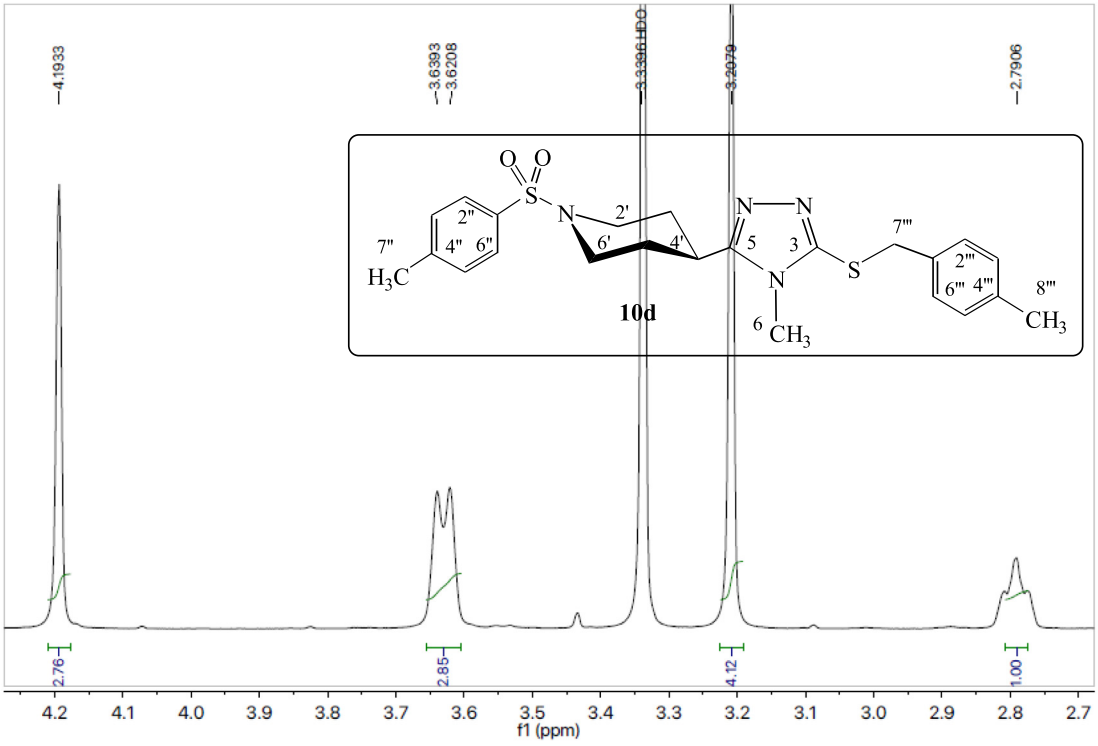

Fig. 3 ^{1}H NMR spectrum (deshielded aliphatic) of compound **10d.**

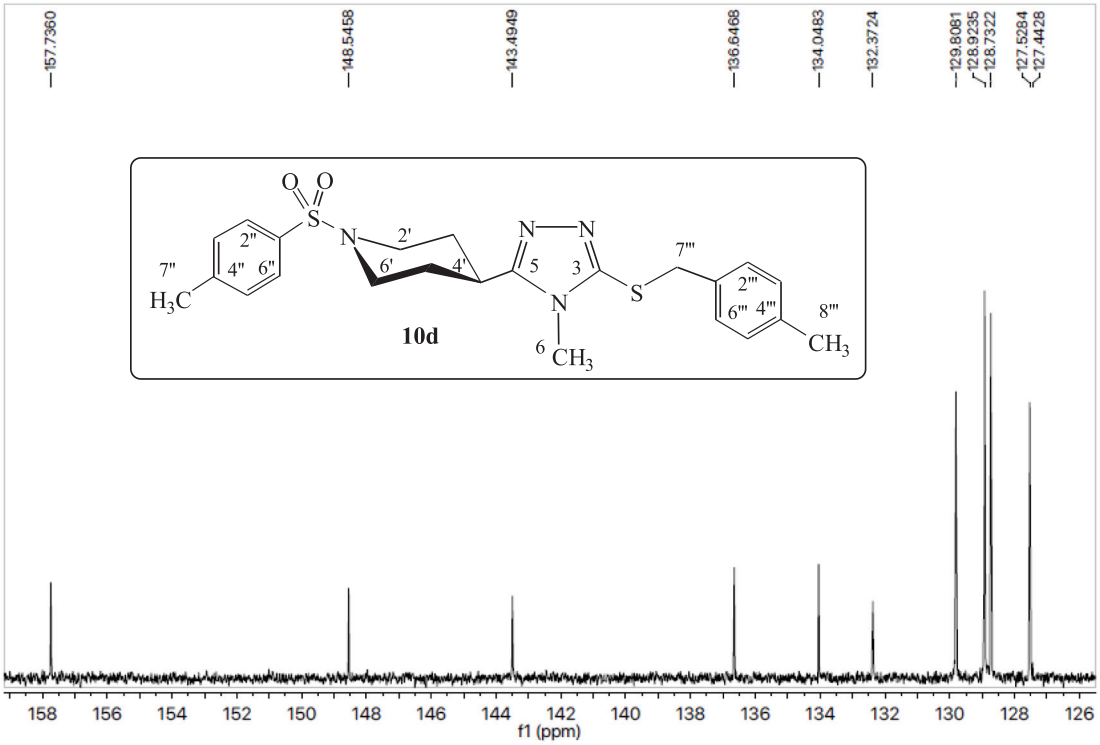

Fig. 4 ^{13}C NMR spectrum (aromatic) of compound **10d.**

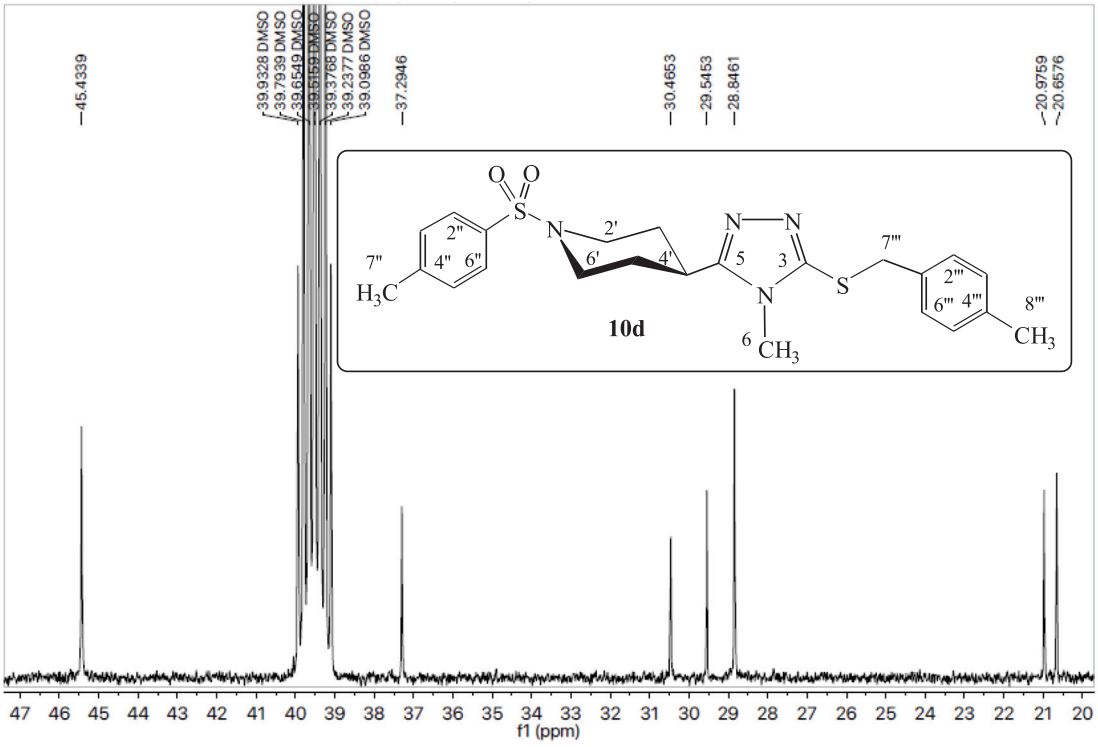

Fig. 5 ^{13}C NMR spectrum (aliphatic) of compound **10d.**

Table 1 AChE and α-Glucosidase inhibition activity of **10a-k.**

Compound	AChE Inhibition		α-Glucosidase Inhibition	
	Inhibition (%) at 0.5 mM	IC_{50} (μM)	Inhibition (%) at 0.5 mM	IC_{50} (μM)
10a	63.24 ± 1.46	0.251 ± 1.24	52.36 ± 1.67	452.75 ± 1.27
10b	87.23 ± 1.12	0.528 ± 0.92	85.35 ± 1.39	56.43 ± 1.13
10c	87.95 ± 1.24	0.537 ± 0.76	82.16 ± 1.74	82.53 ± 1.43
10d	76.52 ± 1.67	0.158 ± 1.22	62.81 ± 1.45	213.62 ± 1.24
10e	64.82 ± 1.46	0.250 ± 1.15	65.34 ± 1.73	325.14 ± 1.36
10f	58.93 ± 1.58	0.339 ± 1.21	62.57 ± 1.72	379.62 ± 1.45
10 g	65.42 ± 1.35	0.262 ± 1.13	62.37 ± 1.57	397.26 ± 1.32
10 h	79.75 ± 1.49	0.115 ± 1.14	76.74 ± 1.81	154.26 ± 1.26
10i	77.42 ± 1.56	0.135 ± 1.31	71.54 ± 1.57	192.43 ± 1.24
10j	87.18 ± 1.23	0.031 ± 0.85	68.87 ± 1.62	317.84 ± 1.32
10 k	90.46 ± 1.21	0.169 ± 0.97	75.21 ± 1.53	413.61 ± 1.29
Standard	**91.27 ± 1.17**[a]	**0.04 ± 0.001**[a]	**65.73 ± 1.93**[b]	**375.82 ± 1.76**[b]

Note: a = Eserine, b = Acarbose.

meta substituted in the mono-halo-benzyl substituents whereas 4-fluorobenzyl bearing molecules were the exception. The only molecule bearing dichloro benzyl moiety remained the most efficient compound against AChE.

Lineweaver-Burk and Michaelis Menten equation was used to determine the value of K_i and type of inhibition at eight different concentrations both in the presence and in absence of triazole derivatives (Table 2 and Figs. 6a & 6b). It can be suggested that derivative 10 k inhibited the AChE un-competitively by binding AChE and AChEI complex reversibly with weak interactions. Furthermore, its K_i value was determined as 0.084 ± 0.05 μM. Literature reported that many neurodegenerative disorders such as Parkinson's disease, Lewy body dementia, myasthenia gravis, and glaucoma especially AD could be treated by cholinesterase inhibitors In another study, (Shelke et al., 2015) investigated water-soluble triazole substituted metal-free and metallo-phthalocyanines for AChE inhibition potential. In line with our findings, 4a phthalocyanine having 0.040 μM IC_{50} was active against AChE which was 1.5-fold active as compared to standard.

The whole series of derivatives were active against the α-glucosidase enzyme (Table 2, Fig. 7). Most of the compounds among the series were active and were better inhibitors than that of the reference standard. The excellent activity was possessed by two compounds, **10b** (bearing 2-methylbenzyl moiety) and **10c** (bearing 3-methylbenzyl moiety). Among the

Table 2 Kinetic studies of triazole derivative (**10a-k**) for AChE.

Sr. No.	Triazole derivative	Type of inhibition	K_i (μM)
	Std drug	Un-competitive	0.018 ± 1.00
	10a	Mixed type	0.211 ± 0.85
	10b	Mixed type	0.492 ± 0.75
	10c	Mixed type	0.548 ± 0.50
	10d	Mixed type	0.198 ± 1.50
	10e	Mixed type	0.248 ± 1.80
	10f	Competitive	0.156 ± 1.75
	10 g	Mixed type	0.251 ± 0.25
	10 h	Un-competitive	0.557 ± 0.50
	10i	Mixed type	0.124 ± 2.5
	10j	Un-competitive	0.015 ± 1.25
	10 k	Un-competitive	0.084 ± 0.05

methyl benzyl substituents, the most active ones were *ortho* and *meta*-substituted molecules while *ortho*-substituted in chlorobenzyl substituents, *meta*-substituted in bromobenzyl substituents, ortho and *meta* in the mono-halo benzyl substituents whereas derivatives bearing unsubstituted benzyl moiety and di chlorobenzyl moiety were found to be the least active ones. Triazole due to its poor basicity as compared to other azaheterocycles is not protonated at physiological pH. The better inhibition potential of derivative compounds might be due to excellent mimic partial positive charge at the anomeric carbon in the transition state of glucosidase catalyzed reaction in non-protonated sp^2-hybridized nitrogen atoms of triazole derivative than corresponding basic nitrogen of iminosugars. Similar to our findings, it has been reported that several triazole derivatives showed an inhibitory

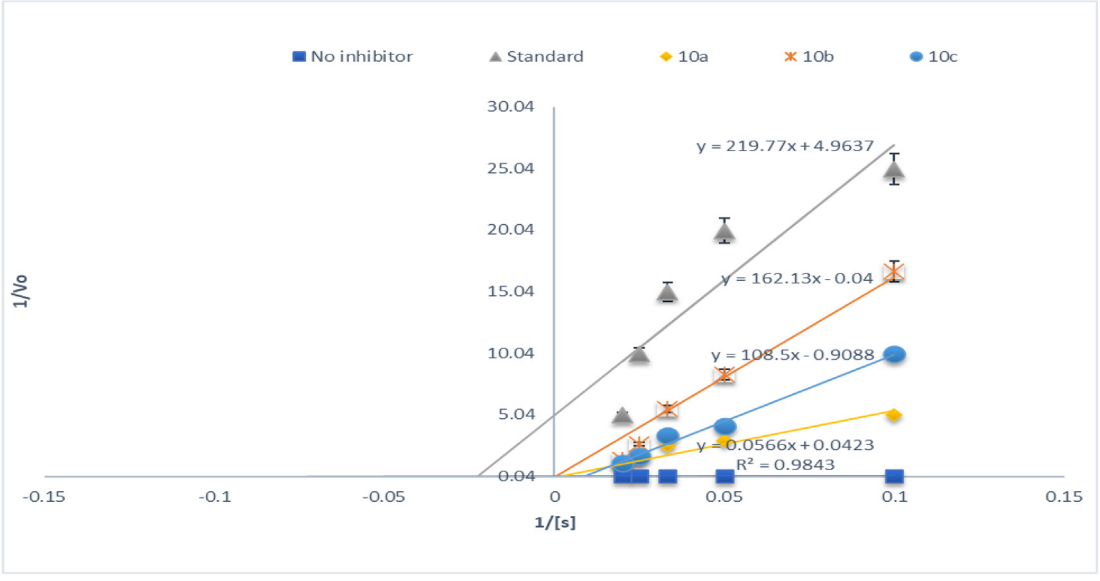

Fig. 6a AChE inhibition of synthesized compounds (**10a-10c**).

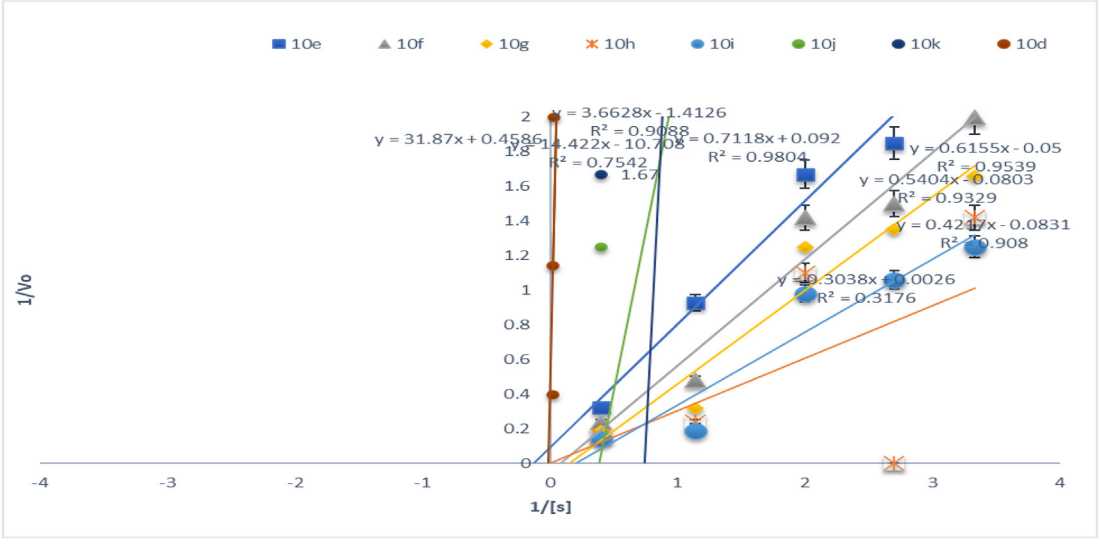

Fig. 6b AChE inhibition of synthesized compounds (**10d-10 k**).

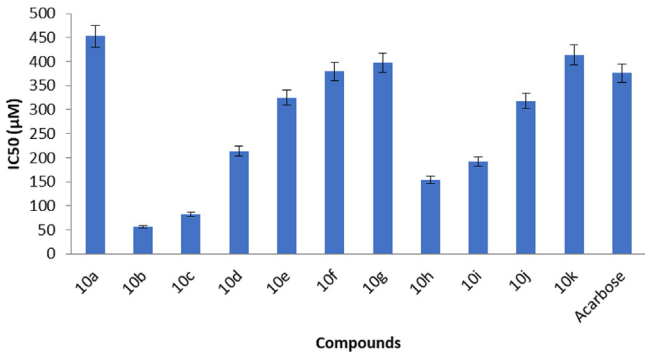

Fig. 7 α-Glucosidase inhibition of synthesized compounds (**10a-k**).

effect against α-glucosidase among which 10b showed promising results and was considered as the most active analog with IC_{50} value of 14.2 μM (Taslimi et al., 2017). Whereas compound 6 showed contrary results due to a low IC_{50} value of 218.1 μM. Similarly, (Ye et al., 2019) determined the antidiabetic potential of xanthone triazole derivatives by inhibiting the α-glucosidase and glucose uptake in $HepG_2$ cells. They reported that compound 5e was found to be most potent having 2.06 μM IC_{50} than parental (1,3-dihydroxyxanthone IC_{50} = 160.8 μM) and 1-deoxynojirimycin (Std. IC_{50} = 59.5 μM). The position of different substituents in 1,2,4-triazole analogs (**10**a-k) helped to establish SAR. *In-vitro* studies have indicated that chloro and fluoro groups present at R_2 and R_3 positions in derivatives best inhibit the activities of both AChE and α-glucosidase. The reason might be due to the presence of chloro and fluoro groups as a substituent on triazole ring have a negative inductive effect causing destabilization of the triazole ring resulting in enhanced activity of 1,2,4-triazole analogs. The compounds 10 k, 10j, 10b, and 10c are the most active and presented the most potent inhibitory potential as compared to others. When all 1,2,4-triazole analogs (**10**a-k) were examined, it was observed that chloro, fluoro and methyl groups containing 1,2,4-triazole analogs (**10**a-k) are the most active compounds. The findings revealed that the triazole analogs prepared in the present investigation showed promising biological activity (Hassan and Arshad, 2022; Tegegne et al., 2020; Shadrach et al., 2020), which have potential for partical application.

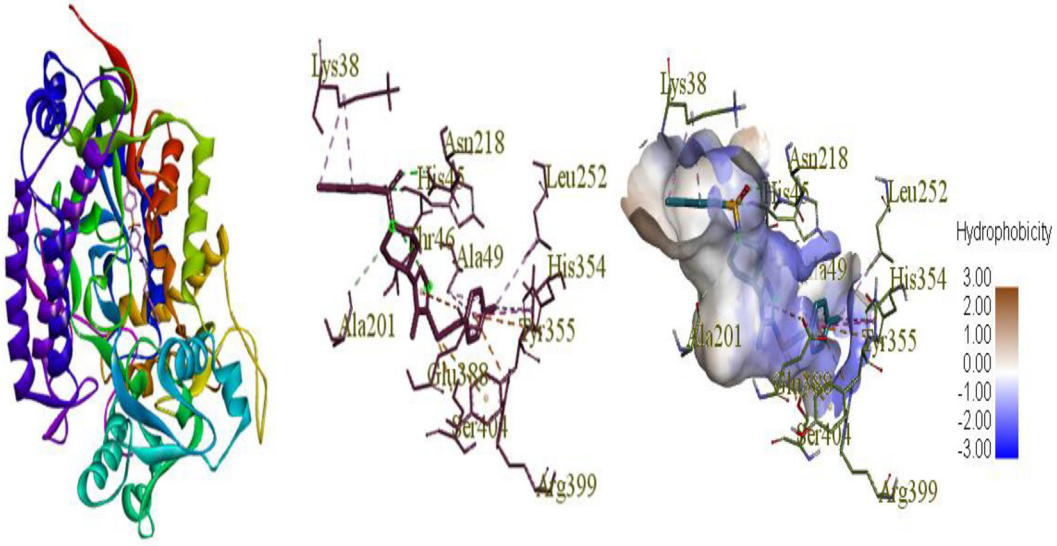

Fig. 8 Binding modes of compound 10j in acetyl cholinesterase (PDB ID:1NEN). Dotted lines presented the hydrogen bonds.

Table 3 Molecular Docking results of compound 10j docked into PDB ID:1NEN.

Ligand	Binding affinity, ΔG (Kcal/mol)	Hydrogen Bonding			Types of Interactions Hydrophobic			Electrostatic		
		Amino acids	Type	Distance	Amino acids	Distance	Type	Amino acids	Distance	Type
Ligand 10j	−9.9	HIS 45 THR 46 ASN 218 ALA 201	Conventional Conventional Conventional C—H bond	2.183 2.647 2.171 3.795	HIS 354 ALA 49 LEU 252 LYS 38 HIS 354 ALA49 LYS 38	5.053 4.292 5.115 4.502 4.934 4.143 4.518	Pi-Pi *T*-shaped Alkyl Alkyl Alkyl Pi-Alkyl Pi-Alkyl Pi-Alkyl	HIS 354 ARG 399 GLU 388	4.4154 4.4118 4.5183	Pi-Cation Pi-Cation Pi-Anion

3.3. Molecular docking simulation

Docking imitations of applicant ligands with AChE co-crystal structure (PDB ID:1NEN) using Auto dock tools predicted that the compound has a value of binding affinity of −9.9 kcal/mol which is the best binding score (Taslimi et al., 2017; Pradhan and Vishwakarma, 2020). The detailed analysis along with types of bonds with their distances formed between the amino acids was provided in Table 3. Drug-target interactions were assumed in the provision of interfacing amino acids fragments, hydrogen bonding, docking energy investigation, presumed binding sites and peculiarities of active site amino acid residues (Fig. 8). Total binding strength is a consequence of different kinds of bonds inclusive of ionic, hydrophobic interactions, Vander Waals forces and hydrogen bonds which are the promoter. Compound (10j) showed conventional hydrogen bonding interactions with amino acid HIS 45, THR 46, ASN 218, ALA 201 and electrostatic interaction with HIS 354, ARG 399, GLU 388 (Virk et al., 2019). It has convenient van der Waals interactions with HIS 354, ALA 49, LEU 252, LYS 38, HIS 354, ALA49, LYS 38 (Ye et al., 2016). In the form of numerous types such as Pi-Pi *T*-shaped, Alkyl and Pi-Alkyl (Yin et al., 2009). All these interactions with certain amino acids occurred at different distances are shown in Table 3.

4. Conclusion

As a result, 1,2,4 triazole derivatives (10a-k) are stronger inhibitors in very low concentrations by the attachment of functional electronegative groups such as -F and -Cl to a triazole ring. As these compounds have an electron density, can inhibit AChE and α-glucosidase by getting them simpler to attach to the functional groups of amino acids. Different inhibitors of these enzyme classes are in clinical practice but are riddled with efficacy, potency and safety challenges. It is concluded from the results of the present study that novel triazole derivatives (10b, 10j and 10 k) are the candidate drugs with anticholinergic and antidiabetic potential for the treatment of some diseases like type 2 DM, dementia, altitude (mountain) sickness and AD. The identified derivatives may be subjected to further analysis by pharmacological industries to check out their use as new drug candidates.

Funding

This research was funded by Princess Nourah bint Abdulrahman University Researchers Supporting Project number (PNURSP2023R18), Princess Nourah bint Abdulrahman University, Riyadh, Saudi Arabia.

Declaration of Competing Interest

The authors declare that they have no known competing financial interests or personal relationships that could have appeared to influence the work reported in this paper.

Acknowledgments

The authors express their gratitude to Princess Nourah bint Abdulrahman University Researchers Supporting Project number (PNURSP2023R18), Princess Nourah bint Abdulrahman University, Riyadh, Saudi Arabia. Research services and analytical facilities provided by Central Hi-Tech Laboratory, Govt. College University, Faisalabad is thankfully acknowledged.

Appendix A. Supplementary material

Supplementary data to this article can be found online at https://doi.org/10.1016/j.arabjc.2023.104626.

References

Akocak, S., Taslimi, P., Lolak, N., Işık, M., Durgun, M., Budak, Y., Türkeş, C., Gülçin, İ., Beydemir, Ş., 2021. Synthesis, characterization, and inhibition study of novel substituted phenylureido sulfaguanidine derivatives as α-glycosidase and cholinesterase inhibitors. Chem. Biodivers. 18 (4), e2000958.

M. Asif, Abida, M.T. Alam, Diverse chemical and biological potentials of various pyridazine and pyridazinone derivatives, Chemistry International 5(3) (2019) 206-231.

Avula, S.K., Khan, A., Rehman, N.U., Anwar, M.U., Al-Abri, Z., Wadood, A., Riaz, M., Csuk, R., Al-Harrasi, A., 2018. Synthesis of 1H–1, 2, 3-triazole derivatives as new α-glucosidase inhibitors and their molecular docking studies. Bioorg. Chem. 81, 98–106.

Bechara, W.S., Khazhieva, I.S., Rodriguez, E., Charette, A.B., 2015. One-pot synthesis of 3, 4, 5-trisubstituted 1, 2, 4-triazoles via the addition of hydrazides to activated secondary amides. Org. Lett. 17 (5), 1184–1187.

Bitla, S., Gayatri, A.A., Puchakayala, M.R., Bhukya, V.K., Vannada, J., Dhanavath, R., Kuthati, B., Kothula, D., Sagurthi, S.R., Atcha, K.R., 2021. Design and synthesis, biological evaluation of bis-(1, 2, 3-and 1, 2, 4)-triazole derivatives as potential antimicrobial and antifungal agents. Bioorg. Med. Chem. Lett. 41, 128004.

G.M. Bousada, B.L. de Sousa, G. Furlani, A.P. Agrizzi, P.G. Ferreira, J.P.V. Leite, T.A.d.O. Mendes, E.V. Varejão, E.J. Pilau, M.H. Dos Santos, Tyrosol 1, 2, 3-triazole analogues as new acetylcholinesterase (AChE) inhibitors, Computational Biology and Chemistry 88 (2020) 107359.

Castaneda, C.A., Cortes-Funes, H., Gomez, H.L., Ciruelos, E.M., 2010. The phosphatidyl inositol 3-kinase/AKT signaling pathway in breast cancer. Cancer Metastasis Rev. 29 (4), 751–759.

Deeba, F., Abbas, N., Butt, M.T., Khan, R.A., Muneeb, M., 2018. Synthesis, characterization and biological activities of 1, 3, 4-oxadiazole derivatives of nalidixic acid and their copper complexes. Chem. Int. 4 (4), 206–215.

Dubovis, M.V., Rudakov, G.F., Kulagin, A.S., Tsarkova, K.V., Popkov, S.V., Goloveshkin, A.S., Cherkaev, G.V., 2018. A new method of synthesis of substituted 1-(1H-imidazole-4-yl)-1H-1,2,3-triazoles and their fungicidal activity. Tetrahedron 74 (6), 672–683.

Duyckaerts, C., Delatour, B., Potier, M.-C., 2009. Classification and basic pathology of Alzheimer disease. Acta Neuropathol. 118 (1), 5–36.

Gaspar, F.V., Azevedo, M.F.M.F., Carneiro, L.S.A., Ribeiro, S.B., Esteves, P.M., Buarque, C.D., 2022. 1,3-Dipolar cycloaddition reactions of enaminones and azides: synthesis of 4-acyl-1,2,3-triazoles and mechanistic studies. Tetrahedron 132856.

Guan, C., Ji, J., Li, Z., Wei, Q., Wu, X., Liu, S., 2022. Facile synthesis of N2-substituted-1,2,3-triazole from aryl ethynylene and azide via a one-pot two-step strategy. Tetrahedron 108, 132670.

Gülçin, İ., Scozzafava, A., Supuran, C.T., Koksal, Z., Turkan, F., Çetinkaya, S., Bingöl, Z., Huyut, Z., Alwasel, S.H., 2016. Rosmarinic acid inhibits some metabolic enzymes including glutathione S-transferase, lactoperoxidase, acetylcholinesterase, butyrylcholinesterase and carbonic anhydrase isoenzymes. J. Enzyme Inhib. Med. Chem. 31 (6), 1698–1702.

Gulçin, İ., Taslimi, P., Aygün, A., Sadeghian, N., Bastem, E., Kufrevioglu, O.I., Turkan, F., Şen, F., 2018. Antidiabetic and antiparasitic potentials: Inhibition effects of some natural antiox-

idant compounds on α-glycosidase, α-amylase and human glutathione S-transferase enzymes. Int. J. Biol. Macromol. 119, 741–746.
Güleç, Ö., Arslan, M., Gencer, N., Ergun, A., Bilen, C., Arslan, O., 2017. Synthesis and carbonic anhydrase inhibitory properties of new spiroindoline-substituted sulphonamide compounds. Arch. Physiol. Biochem. 123 (5), 306–312.
Güleç, Ö., Türkeş, C., Arslan, M., Demir, Y., Yeni, Y., Hacımüftüoğlu, A., Ereminsoy, E., Küfrevioğlu, Ö.İ., Beydemir, Ş., 2022. Cytotoxic effect, enzyme inhibition, and in silico studies of some novel N-substituted sulfonyl amides incorporating 1, 3, 4-oxadiazol structural motif. Mol. Divers., 1–21
Gümüş, M., Babacan, Ş.N., Demir, Y., Sert, Y., Koca, İ., Gülçin, İ., 2022. Discovery of sulfadrug–pyrrole conjugates as carbonic anhydrase and acetylcholinesterase inhibitors. Arch. Pharm. 355 (1), 2100242.
Haddad, S., Boudriga, S., Akhaja, T.N., Raval, J.P., Porzio, F., Soldera, A., Askri, M., Knorr, M., Rousselin, Y., Kubicki, M.M., 2015. A strategic approach to the synthesis of functionalized spirooxindole pyrrolidine derivatives: in vitro antibacterial, antifungal, antimalarial and antitubercular studies. New J. Chem. 39 (1), 520–528.
Hao, W., Chen, J., Zhang, Y., Mou, T., Wang, J., Zhang, C., Gu, S., Zhao, T., Sun, Y., Cui, M., Wei, B., 2023. Integration of metabolomics and network pharmacology to validate the mechanism of Schisandra chinensis(Turcz.)Baill - Acorus tatarinowii Schott ameliorating the Alzheimer's disease by regulating the aromatase activity to affect local estrogen in brain of AD model rats. Arab. J. Chem. 16, (2) 104457.
Hassan, S.M., Arshad, M., 2022. Nutra-pharmaceutical potential evaluation of Trignollafoenum graecum seeds extracts in different solvents. Chem. Int. 8 (1), 23–32.
Honka, M.-J., Latva-Rasku, A., Bucci, M., Virtanen, K.A., Hannukainen, J.C., Kalliokoski, K.K., Nuutila, P., 2018. Insulin-stimulated glucose uptake in skeletal muscle, adipose tissue and liver: a positron emission tomography study. Eur. J. Endocrinol. 178 (5), 523–531.
Isik, Z., Baldow, C., Cannistraci, C.V., Schroeder, M., 2015. Drug target prioritization by perturbed gene expression and network information. Sci. Rep. 5 (1), 1–13.
Isik, A.T., Soysal, P., Solmi, M., Veronese, N., 2019. Bidirectional relationship between caregiver burden and neuropsychiatric symptoms in patients with Alzheimer's disease: a narrative review. Int. J. Geriatr. Psychiatry 34 (9), 1326–1334.
Jha, K.K., Samad, A., Kumar, Y., Shaharyar, M., Khosa, R.L., Jain, J., Kumar, V., Singh, P., 2010. Design, synthesis and biological evaluation of 1, 3, 4-oxadiazole derivatives. Eur. J. Med. Chem. 45 (11), 4963–4967.
Kousar, K., Majeed, A., Yasmin, F., Hussain, W., Rasool, N., 2020. Phytochemicals from selective plants have promising potential against SARS-CoV-2: investigation and corroboration through molecular docking, MD simulations, and quantum computations. Biomed Res. Int. 2020.
Laube, B.L., 2002. Advances in treating diabetes with aerosolized insulin. Diabetes Technol. Ther. 4 (4), 515–518.
Li, Z.-H., Yin, L.-Q., Zhao, D.-H., Jin, L.-H., Sun, Y.-J., Tan, C., 2023. SAR studies of quinoline and derivatives as potential treatments for Alzheimer's disease. Arab. J. Chem. 16, (2) 104502.
Li, J., Zhang, J., 2021. The antibacterial activity of 1, 2, 3-triazole-and 1, 2, 4-triazole-containing hybrids against Staphylococcus aureus: An updated review (2020-present). Curr. Top. Med. Chem.
Mitsumori, T., Bendikov, M., Sedó, J., Wudl, F., 2003. Synthesis and properties of novel highly fluorescent pyrrolopyridazine derivatives. Chem. Mater. 15 (20), 3759–3768.
Muhammad, I., Pandian, S., Hopper, W., 2020. Antibacterial and antioxidant activity of p-quinone methide derivative synthesized from 2, 6-di-tert-butylphenol. Chem. Int. 6 (4), 260–266.
Pathak, P., Novak, J., Shukla, P.K., Grishina, M., Potemkin, V., Verma, A., 2021. Design, synthesis, antibacterial evaluation, and computational studies of hybrid oxothiazolidin–1, 2, 4-triazole scaffolds. Arch. Pharm. 354 (6), 2000473.
Pradhan, A., Vishwakarma, S., 2020. Synthesis of quinolone derivatives and their molecular docking for antiepileptic activity. Chem. Int. 6 (4), 224–231.
Sacchetti, A., Urra Mancilla, C., Colombo Dugoni, G., 2022. Synthesis of DPA-triazole structures and their application as ligand for metal catalyzed organic reactions. Tetrahedron 104, 132581.
Shadrach, I., Banji, A., Adebayo, O., 2020. Nutraceutical potential of ripe and unripe plantain peels: A comparative study. Chem. Int. 6 (2), 83–90.
Shelke, G.M., Rao, V.K., Jha, M., Cameron, T.S., Kumar, A., 2015. Microwave-assisted catalyst-free synthesis of substituted 1, 2, 4-triazoles. Synlett 26 (03), 404–407.
Suhail, M., Ali, I., 2020. Gas chromatography: A tool for drug analysis in biological samples. Chem. Int. 6 (4), 277–294.
Tao, Y., Zhang, Y., Cheng, Y., Wang, Y., 2013. Rapid screening and identification of α-glucosidase inhibitors from mulberry leaves using enzyme-immobilized magnetic beads coupled with HPLC/MS and NMR. Biomed. Chromatogr. 27 (2), 148–155.
Taslimi, P., Akıncıoglu, H., Gülçin, İ., 2017. Synephrine and phenylephrine act as α-amylase, α-glycosidase, acetylcholinesterase, butyrylcholinesterase, and carbonic anhydrase enzymes inhibitors. J. Biochem. Mol. Toxicol. 31 (11), e21973.
Taslimi, P., Köksal, E., Gören, A.C., Bursal, E., Aras, A., Kılıç, Ö., Alwasel, S., Gülçin, İ., 2020. Anti-Alzheimer, antidiabetic and antioxidant potential of Satureja cuneifolia and analysis of its phenolic contents by LC-MS/MS. Arab. J. Chem. 13 (3), 4528–4537.
Taslimi, P., Işık, M., Türkan, F., Durgun, M., Türkeş, C., Gülçin, İ., Beydemir, Ş., 2021. Benzenesulfonamide derivatives as potent acetylcholinesterase, α-glycosidase, and glutathione S-transferase inhibitors: biological evaluation and molecular docking studies. J. Biomol. Struct. Dyn. 39 (15), 5449–5460.
Tegegne, B., Belay, A., Gashaw, T., 2020. Nutritional potential and mineral profiling of selected rice variety available in Ethiopia. Chem. Int. 6 (1), 21–29.
Türkeş, C., Akocak, S., Işık, M., Lolak, N., Taslimi, P., Durgun, M., Gülçin, İ., Budak, Y., Beydemir, Ş., 2021. Novel inhibitors with sulfamethazine backbone: synthesis and biological study of multi-target cholinesterases and α-glucosidase inhibitors. J. Biomol. Struct. Dyn., 1–13
Virk, N., Abbasi, M., Siddiqui, S., Ashraf, A., Iqbal, J., Rasoo, S., Khalid, H., Laulloo, S., Khan, S., Shah, S., 2019. Biological screening and docking studies of unique hybrids synthesized by conventional versus microwave assisted techniques. Trop. J. Pharm. Res. 18 (5), 1109–1117.
Ye, N., Chen, H., Wold, E.A., Shi, P.-Y., Zhou, J., 2016. Therapeutic potential of spirooxindoles as antiviral agents. ACS Infect. Dis. 2 (6), 382–392.
Ye, Y., Ngo, H.H., Guo, W., Chang, S.W., Nguyen, D.D., Liu, Y., Nghiem, L.D., Zhang, X., Wang, J., 2019. Effect of organic loading rate on the recovery of nutrients and energy in a dual-chamber microbial fuel cell. Bioresour. Technol. 281, 367–373.
Yin, P., Ma, W.-B., Chen, Y., Huang, W.-C., Deng, Y., He, L., 2009. Highly efficient cyanoimidation of aldehydes. Org. Lett. 11 (23), 5482–5485.